A Switched Systems Approach Based on Changing Muscle Geometry of the Biceps Brachii During Functional Electrical Stimulation

Courtney A. Rouse, Victor H. Duenas, Christian Cousin, Anup Parikh, and Warren E. Dixon

Abstract—**Functional electrical stimulation (FES) is commonly used for people with neurological conditions. As the muscle geometry changes (i.e., muscle lengthening/shortening), the force induced by static electrode placement may also change. Experimental results indicate that muscle forces can be increased by spatially switching stimulation as the muscle geometry changes with joint angle. In this letter, an electric field is switched between multiple electrodes placed across the biceps brachii to track a desired trajectory. A switched systems approach is used to develop a position-based switching law, including a switched robust sliding mode controller that successfully tracks the desired angular trajectory about the elbow, despite changes in muscle geometry. Lyapunov-based methods for switched systems are used to prove global exponential tracking. Experimental results from nine able-bodied subjects are presented and the developed control system achieves an average position and velocity error of -0.21 ± 1.17 deg and -0.43 ± 5.38 deg/s, respectively, and, on average, reduces fatigue by 13.6%, as compared to traditional single-electrode methods, demonstrating the performance of the uncertain nonlinear switched control system.**

Index Terms—**Functional electrical stimulation (FES), human-robot interaction, Lyapunov methods, rehabilitation robotics, switched control.**
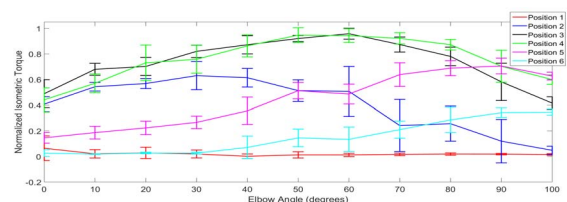
Fig. 1. Normalized isometric elbow torque for six electrode locations across the biceps brachii. Position 1-6 refer to electrode placement, distally to proximally. The normalized torque data is averaged over five trials with standard deviation bars and linearly interpolated to show trends. Normalization was based on the maximum isometric torque produced throughout each trial. This data establishes that switching stimulation sites with elbow angle could yield maximum torque production over the entire range of motion.

I. INTRODUCTION

MUSCLE contractions induced via neuromuscular electrical stimulation (NMES) that assist in functional limb movement is known as functional electrical stimulation (FES). Evidence in literature has well established that electrode placement affects motor unit recruitment and that the generated force varies with changing muscle geometry (i.e., muscle lengthening or shortening). In particular, [1] and [2] indicates that electrode proximity to the motor point (where the motor branch of a nerve enters the muscle belly) is critical for optimal force production. Muscle geometry changes with limb position and orientation, so the motor point, and thus the optimal stimulation site, is also expected to change. Altering muscle length by changing the joint angle varies the position of muscle fibers with respect to the electrodes, influencing the contribution of cutaneous input (sensory receptors) to the elicited contraction [3]. Manipulating the joint angle to cause a change in muscle geometry could maximize NMES benefits in a more practical way than high stimulation input or manually moving electrodes [4]. Initial experiments by the authors show that the normalized isometric elbow torque changes with limb position and that varying the stimulation site would be beneficial (Figure 1). Maximizing torque by switching among electrodes spatially distributed across the muscle motivates the open question of how to perform closed-loop state-dependent switching across a muscle.

Although no previous methods perform state-dependent switching across a muscle group, time-based switching methods have been developed to reduce muscle fatigue [5]–[7]. One approach to vary the stimulation site during FES is to use an electrode array to switch between different muscle groups [8]–[15]; however, these previous works do not prove

stability or guarantee performance for a switched closed-loop controller to rotate the forearm about the elbow.

Previous FES-cycling control studies (see [16]–[20]) used a switched control input that alternated stimulation across different muscle groups according to a predefined open-loop stimulation pattern. In comparison to other cycling literature, the results in [21] and [22] develop closed-loop controllers where the stability of the controller is analyzed through a position-based switched systems analysis; however none involve spatially switching across a single muscle group where each subsystem is stable.

This letter, and the preliminary efforts in [23], consider a nonlinear model of the forearm rotating about the elbow. The scalar second order dynamics are uncertain, nonlinear, and subject to bounded exogenous disturbances (e.g., muscle spasticity, changing loads, etc.). A sliding mode controller is designed for the uncertain nonlinear system with autonomous state-dependent switching. Via Lyapunov methods, stability of the switched system and global exponential tracking of each subsystem (i.e., stimulation site) of the desired trajectory is obtained, provided sufficient gain conditions are satisfied. The same Lyapunov candidate and analysis applies for all subsystems so the Lyapunov derivatives of all subsystems share a common bound, proving global exponential tracking for the entire system. In comparison to the preliminary results in [23], this letter has further developed mathematical analysis and experimental results from ten able-bodied subjects to demonstrate the tracking performance of the switching controller and results from five subjects to demonstrate the advantageous reduction in fatigue.

II. MODEL

A. Testbed and Human Dynamic Model

The developed controller is focused on the biceps brachii as an example muscle where the geometry changes significantly throughout the range of motion. Consider the dynamics of the forearm trajectory as

$$M\ddot{q}(t) + V(q(t), \dot{q}(t))\dot{q}(t) + G(q(t))$$
$$-\tau_b(\dot{q}(t)) - \tau_d(t) = \tau_m(t), \tag{1}$$

where $q : \mathbb{R}_{>0} \to Q$ denotes the angular forearm position about the elbow joint, and $Q \subseteq \mathbb{R}$ denotes the set of forearm angles. The states q and $\dot{q}$ are assumed to be measurable. Also in (1), $M \in \mathbb{R}_{>0}$ is a positive constant that denotes the inertial effects; $V : Q \times \mathbb{R} \to \mathbb{R}$ denotes centripetal and Coriolis effects; and $G : Q \to \mathbb{R}$ denotes gravitational effects. Torques applied about the elbow by viscous damping of the testbed's hinge are denoted by $\tau_b : \mathbb{R} \to \mathbb{R}$, $\tau_d : \mathbb{R}_{>0} \to \mathbb{R}$ denotes unknown disturbances (e.g., spasticity or changes in load), and $\tau_m : \mathbb{R}_{>0} \to \mathbb{R}$ denotes torques applied about the elbow joint axis (e.g., muscle contractions).

B. Switched System Model

Consider multiple electrodes placed along the biceps as $w \in \mathbb{N}$ distinct channels, wherethe torque from (1) is generated by applying a potential field across a channel as

$$\tau_m(t) = \Omega_i(q(t), \dot{q}(t))u(t), \tag{2}$$

where $i \in S$ denotes the ith channel and $S \triangleq \{1, 2, \ldots, w\}$ denotes a finite indexed set of w subsystems. The electrical stimulation intensity is denoted as $u : \mathbb{R}_{>0} \to \mathbb{R}$ and $\Omega_i : Q \times \mathbb{R} \to \mathbb{R}_{>0}$ denotes an unknown auxiliary function of the elbow's angular position and velocity that varies with time and relates the stimulation intensity applied to the ith stimulation channel to the torque produced by the activated sensory-motor structures, (see [7], [24]). Based on [7], [23]–[25], Ω_i is a non-zero, positive, bounded function and the first two partial derivatives with respect to time are assumed to exist and be bounded for bounded states q and $\dot{q}$.

The stimulation of the biceps muscle is generated by the control input and applied to each subsystem at the joint angle for which elbow torque is maximized. Switching the control input in this way yields an autonomous, state-dependent, switched control system [26]. Subsystem i is stimulated when $q \in Q_i$, $i \in S$ where $\{Q_i\}_1^w$ partitions Q. Thus, stimulation is never applied to any two locations at the same time. Substituting (2) into (1) yields

$$M\ddot{q}(t) + V(q(t), \dot{q}(t))\dot{q}(t) + G(q(t))$$
$$-\tau_b(\dot{q}(t)) - \tau_d(t) = \Omega_{\sigma(q)}u(t), \tag{3}$$

where $\sigma : Q \to S$ is the right continuous switching signal indicating which channel is being stimulated. Stimulation is applied throughout the arm trajectory; however, some stimulation channels may never be excited. Since only one electrode pair is stimulated at a time, there are $w - 1$ possibilities at every switching event. Since Ω_i is bounded for all $i \in S$, Ω_σ is bounded. The model in (3) has the following properties [24], [27], [28]: **Property 1.** $c_1 \leq \Omega_i(q(t), \dot{q}(t)) \leq c_2, \forall i \in S$; $c_1, c_2 \in \mathbb{R}_{>0}$ are known constants. **Property 2.** $c_m \leq M \leq c_M$; $c_m, c_M \in \mathbb{R}_{>0}$. **Property 3.** $|V(q(t), \dot{q}(t))| \leq c_V|\dot{q}|$; $c_V \in \mathbb{R}_{>0}$ is a known constant. **Property 4.** $|G(q(t))| \leq c_G$; $c_G \in \mathbb{R}_{>0}$ is a known constant. **Property 5.** $|\tau_b(\dot{q}(t))| \leq c_b|\dot{q}|$; $c_b \in \mathbb{R}_{>0}$ is a known constant. **Property 6.** $|\tau_d(t)| \leq c_d$; $c_d \in \mathbb{R}_{>0}$ is a known constant.

III. ERROR SYSTEM DEVELOPMENT

The control objective is to track a desired forearm trajectory, quantified by the position tracking error, defined as

$$e_1(t) \triangleq q_d(t) - q(t), \tag{4}$$

where $q_d : \mathbb{R}_{>0} \to \mathbb{R}$ is the desired forearm position, designed so its first and second derivatives exist, and are bounded. Without loss of generality, q_d is designed to monotonically increase, i.e., stopping or changing directions is not desired for the current study, which only focuses on motion that can be induced by stimulation of the biceps. To facilitate the subsequent development, an auxiliary tracking error $e_2 : \mathbb{R}_{>0} \to \mathbb{R}$ is defined as

$$e_2(t) \triangleq \dot{e}_1(t) + \alpha e_1(t), \tag{5}$$

where $\alpha \in \mathbb{R}_{>0}$ is a selectable constant gain. Taking the time derivative of (5), multiplying by M, adding and subtracting e_1, and using (3) and (4) yields

$$M\dot{e}_2(t) = \chi(q(t), \dot{q}(t), t) - e_1(t) - \Omega_\sigma u(t), \tag{6}$$

where the auxiliary term $\chi : Q \times \mathbb{R} \times \mathbb{R}_{>0} \to \mathbb{R}$ is defined as

$$
\begin{aligned}
\chi(q(t), \dot{q}(t), t) \triangleq\ & M(\ddot{q}_d(t) + \alpha \dot{e}_1(t)) \\
& + V(q(t), \dot{q}(t))\dot{q}(t) + G(q(t)) \\
& - \tau_b(\dot{q}(t)) - \tau_d(t) + e_1(t).
\end{aligned} \tag{7}
$$

From Properties 3-6, χ can be bounded as

$$
|\chi(q(t), \dot{q}(t), t)| \leq c_3 + c_4 \parallel z(t) \parallel + c_5 \parallel z(t) \parallel^2, \tag{8}
$$

where c_3, c_4, $c_5 \in \mathbb{R}_{>0}$ are known constants, $\parallel \cdot \parallel$ denotes the Euclidean norm, and the error vector $z \in \mathbb{R}^2$ is defined as $z(t) \triangleq \begin{bmatrix} e_1(t) & e_2(t) \end{bmatrix}^T$. Based on (6)-(8) and the subsequent stability analysis, the control input is designed as

$$
\begin{aligned}
u(t) \triangleq\ & k_1 e_2(t) \\
& + k_2\Big(c_3 + c_4 \parallel z(t) \parallel + c_5 \parallel z(t) \parallel^2\Big)\mathrm{sgn}(e_2(t)), \tag{9}
\end{aligned}
$$

where $\mathrm{sgn}(\cdot)$ denotes the signum function, k_1, $k_2 \in \mathbb{R}_{>0}$ are constant control gains, and c_3, c_4, c_5 were defined in (8). Substituting (9) into (6) yields

$$
\begin{aligned}
M\dot{e}_2(t) =\ & \chi(q(t), \dot{q}(t), t) - e_1(t) \\
& - \Omega_\sigma \Big[k_1 e_2(t) + k_2\Big(c_3 + c_4 \parallel z(t) \parallel \\
& + c_5 \parallel z(t) \parallel^2\Big)\mathrm{sgn}(e_2(t)) \Big]. \tag{10}
\end{aligned}
$$

IV. STABILITY ANALYSIS

Theorem 1: The controller in (9) yields global exponential tracking in the sense that

$$
\parallel z(t) \parallel \leq \sqrt{\frac{\lambda_2}{\lambda_1}} \parallel z(t_0) \parallel \exp\left[-\frac{1}{2}\lambda_s(t - t_0)\right], \tag{11}
$$

$\forall t \in [t_0, \infty)$, where $t_0 \in \mathbb{R}_{>0}$ is the initial time, and $\lambda_s \in \mathbb{R}_{>0}$ is defined as

$$
\lambda_s \triangleq \frac{1}{\lambda_2} \min(\alpha, c_1 k_1), \tag{12}
$$

provided the following gain condition is satisfied:

$$
k_2 \geq \frac{1}{c_1}, \tag{13}
$$

where c_1 is defined in Property 1.

Proof: See the Appendix. ∎

V. EXPERIMENTS

One female and nine male able-bodied subjects, 20-45 years old, participated in the experiments. All subjects gave written informed consent approved by the University of Florida Institutional Review Board. During the experiments, subjects were instructed to relax and make no volitional effort to assist or inhibit the FES input.

A. Experimental Testbed

A customized testbed, as used in [23], was used for all experiments. An optical digital encoder was coupled at the elbow to continuously measure the angular position and velocity of the forearm. A 27 Watt, brushed, parallel-shaft

gearmotor at the hinge was supplied current by a general purpose linear amplifier interfacing with the data acquisition hardware, which also measured the encoder signal.

Since a biceps curl is only continuous for a certain range of angles, the motor brought the arm from the largest angle of testing (i.e., top of the biceps curl) back to the smallest angle of testing. The motor was also used in the stimulation region,[1] but was not a subsystem of nor had any effect on the analysis of the subsystems in the switched system. The controller was implemented on a personal computer running real-time control software.

A current-controlled stimulator (Hasomed RehaStim) delivered biphasic, symmetric, rectangular pulses to the subject's muscle via self-adhesive, PALS® electrodes.[2] Six 0.6" x 2.75" electrodes representing the six subsystems in this letter's analysis were placed over the biceps between the elbow crease and acromion with the shared reference electrode on the shoulder. Based on comfort and torque levels, the pulse width was fixed at 90 μs with a frequency of 35 Hz for each stimulation channel and the amplitude was determined by the developed feedback controller in (9), saturated at 55 mA, and commanded to the stimulator by the control software.

B. Switching Protocol

Prior to each experiment, a switching map similar to Figure 1 was developed. This data was then used to create a switching law for dynamic experiments so that more effective electrodes were stimulated throughout the arm's range of motion. The midpoints between the angles for which isometric contractions were produced were used as the switching points (i.e., where the switching signal σ changed to a different subsystem).

After the electrodes were placed on the subject's upper arm, the subject was comfortably seated so that the table was chest height. The protocol was conducted on each arm with the arm order selected at random. The desired angular position, q_d, selected as $q_d(t) = \begin{cases} \frac{\pi t}{90} & t \leq 10 \\ \frac{\pi}{90} + \frac{7\pi}{36}\left[1 - \cos\left(\pi \frac{t-10}{10}\right)\right] & t > 10 \end{cases}$, and depicted in Figure 2, consists of a period where the motor brings the arm to 20 degrees, which was found to be the point where stimulation begins to produce a reasonable amount of torque. The developed FES switching control was used to control the arm motion from 20 to 90 degrees. Motor control was used to bring the forearm from 90 degrees back to 20 degrees, where the trajectory was repeated four more times. The control gains introduced in (9), and the constant α introduced in (5), were adjusted to yield acceptable tracking performance with a range of values as follows: $\alpha \in [5, 10]$, $k_1 \in [12, 30]$, $k_2 = 1$.

C. Results

All results represent data taken from the stimulation periods only since the performance of the motor-only section of

---

[1]Stimulation region refers to the region when the biceps are contracting due to FES and the motor is also providing a small open-loop current to offset friction in the motor gear box. The contribution of the motor in the stimulation region is not sufficient to move the arm without FES.

[2]Surface electrodes for this letter were provided compliments of Axelgaard Manufacturing Co., Ltd.
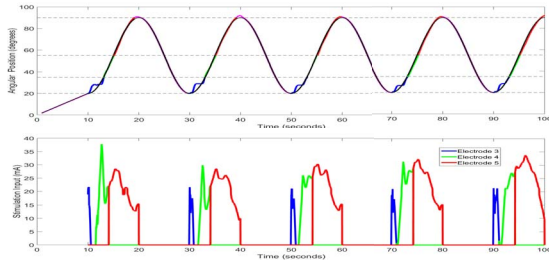
Fig. 2. Desired and actual trajectory for Subject 1, right arm, for five biceps curls is depicted on top with the stimulation intensity below. The solid black line depicts the desired trajectory. The magenta line represents motor-only control regions. The blue, red, and green lines represent actual arm position for each stimulation channel in the FES control region. In general, switching could have occured every 10 degrees with the option of six different channels. However, for this trial, switching only occured at 35 degrees and 55 degrees between three channels, as determined by the pretrial isometric torque experiments. The dotted lines represent the two switching points as well as the angles for which the system changes from using the motor to stimulation, and vice versa. The position-based switching law is identical for all biceps curls in a trial.

TABLE I

MEAN AND STANDARD DEVIATION FOR POSITION AND VELOCITY TRACKING ERROR FOR ALL SUBJECTS

Subject/Arm	Mean Position Error, μ_{e_1} (deg)	St. Dev. Position Error, σ_{e_1} (deg)	Mean Velocity Error, $\mu_{\dot{e}_1}$ (deg/s)	St. Dev. Velocity Error, $\sigma_{\dot{e}_1}$ (deg/s)
1 Right	-1.61	1.53	-0.25	4.33
1 Left	-0.71	1.20	-0.34	4.70
2 Right	1.23	1.52	-0.32	5.03
2 Left	0.18	1.33	-0.39	5.42
3 Right	-0.51	0.91	-0.28	4.15
3 Left	-0.71	1.21	-0.62	5.90
4 Right	0.73	0.98	-0.26	4.88
4 Left	0.11	0.70	-0.40	4.86
5 Right	-0.54	0.76	-0.38	4.93
5 Left	-0.91	0.90	-0.50	5.67
6 Right	-0.32	0.76	-0.37	5.63
6 Left	-0.33	1.07	-0.42	7.19
7 Right	1.16	1.15	-0.28	7.37
7 Left	1.26	1.49	-0.32	7.42
8 Right	-0.37	1.37	-0.64	7.76
8 Left	-1.07	1.14	-0.61	4.58
9 Right	-0.89	1.58	-0.78	4.85
9 Left	-0.41	1.30	-0.60	4.90
Average	-0.21	1.17	-0.43	5.38

the trajectory is not a product of the switching control design (i.e., when $\dot{q} \geq 0$). Table I summarizes the overall position and velocity tracking performance of each subject during stimulation. Figure 2 depicts an example desired and actual trajectory and stimulation input for the right arm of Subject 1.

The tracking results in Table I indicate the performance of the controller. A comparative study was also conducted to examine the effects of the developed electrode switching strategy compared to the typical single electrode strategy, where the channel that was most efficient for the majority of the biceps curl (as per pre-trial experiments depicted in Figure 1) was used throughout. The experiments were completed on a subset of the available participants from the original experiments.[3] The order of the two protocols was selected at random.

---

[3]The left arm of Subject 1 was broken due to an unrelated event, and experiments on that arm were excluded from further experiments.

TABLE II

DIFFERENCE IN POST-TRIAL TORQUE-TIME INTEGRAL FOR ALL SUBJECTS

Subject/Arm	TTI Percent Decrease	Overall Average Muscle Current Percent Decrease	Average Muscle Current Percent Decrease per Electrode
1 Right	12.7%	-1.22%	24.85%
2 Right	-33.5%	4.11%	6.68%
2 Left	14.0%	0.49%	6.92%
4 Right	25.4%	1.66%	24.74%
4 Left	38.4%	27.81%	48.97%
8 Right	28.8%	-13.39%	34.41%
8 Left	5.8%	-6.88%	21.80%
9 Right	0.0%	1.12%	1.65%
9 Left	31.0%	2.39%	15.51%
Average	13.6%	1.79%	20.61%

TABLE III

COMPARISON OF AVERAGE RMS ERRORS FOR POSITION AND VELOCITY TRACKING DURING SWITCHING VS. SINGLE ELECTRODE STIMULATION

	Mean	Std. Deviation
Single Electrode Position RMS Error (deg)	4.40	1.60
Switching Position RMS Error (deg)	4.12	1.76
Single Electrode Velocity RMS Error (deg/s)	7.63	2.05
Switching Velocity RMS Error (deg/s)	7.54	1.69

During a pretrial test with the forearm angle at 30 degrees, the subject's maximum voluntary torque was measured and the current amplitude which produced 30-40% of maximum voluntary torque was recorded, along with the isometric torque produced at that stimulation intensity. Next, the respective protocol (i.e., switching or single electrode) was performed for 10 biceps curls. A post-trial test included 20 seconds of constant stimulation at the same intensity and elbow angle as the pretrial. The torque-time integral (TTI), which measures sustained torque production and was normalized by the pretrial maximum torque, was calculated for both protocols as a commonly used method to quantify fatigue after exercise protocols [6]. The TTI was greater when stimulation was switched along the biceps than when a single electrode was stimulated, for all subjects tested, with the exception of the right arm of Subject 2, as shown in Table II. Position and velocity error, in Table III, was also recorded during the second set of experiments to show that tracking performance was not compromised during switched stimulation.

D. Discussion

The first experimental results demonstrate the exponential tracking performance of the discontinuous switching controller designed in (9), despite parametric uncertainties (e.g., M, ς_i, φ_i, η_i, τ_b) and unknown disturbances (e.g., τ_d, $\dot{\tau}_d$). Errors are likely due to unmodeled effects such as electromechanical delay from activation time to time of muscle force production [29]. The testbed joint also allowed small movements without opposing motor friction, which resulted in practically no additional position error but may have contributed to the larger velocity error.

The range of position and velocity errors are similar to other published FES experiments [7]; however, the wider range of velocity error is likely attributed to a bias in the tuning of control gains towards improving position error, as overshooting the arm's comfortable range of motion presented a potential safety concern.

As shown in Table II, switching amongst electrodes placed across the biceps brachii, according to the forearm angle and torque efficiency, resulted in less fatigue than stimulating one electrode throughout the biceps curls for all but one arm of one subject. To quantify fatigue, the post-trial TTI was compared between switching and non-switching protocols. As shown in Table III, the mean and standard deviation of RMS errors for position and velocity were very similar between switching and single-electrode protocols, showing that the novel switching approach tracks a desired trajectory just as well as single-electrode biceps curls, while reducing fatigue. The last two columns of Table II show the percent decrease in stimulation input overall, and the weighted average percent decrease per electrode. Although the overall percent decrease in stimulation intensity between single electrode and switching protocols does not correlate with the reduction in fatigue, column four shows that no single electrode recieves as high of stimulation intensity for as long a duration as in single electrode stimulation. Thus, no one part of the biceps is being fatigued as much as during single electrode stimulation.

Experiments on able-bodied subjects validate the stability of the FES controller; however, the ultimate application for the developed controller is for people with neurological disorders, which may present additional challenges, such as variation in patient sensitivity to FES. Although unintentional contribution to muscle force production during able-bodied experiments is often a concern in the validity of FES research, the subjects in this letter were not shown the desired or actual trajectory so any unintentional contribution will not necessarily improve tracking and, thus, can be treated as a disturbance.

VI. CONCLUSION

An uncertain, nonlinear model for FES forearm movement about the elbow was presented which includes the effects of a switched control input with unknown disturbances. Because the muscle geometry of the biceps changes as the forearm moves, a switching strategy was developed that applies FES along the biceps brachii, based on the angular position of the forearm. The switched sliding mode controller yields global exponential tracking of a desired forearm trajectory, provided sufficient gain conditions are satisfied. The control design was validated in experiments with ten able-bodied subjects, where average position and velocity tracking errors of -0.21 ± 1.17 deg and -0.43 ± 5.38 deg/s, respectively, were demonstrated. Switching also resulted in less fatigue, evaluated using a post-trial TTI. The results indicate that by switching the stimulation channel with elbow position based on isometric torque data can reduce fatigue and yield similar tracking compared to traditional single channel stimulation methods. Additional effects to be explored, such as arm orientation (vertical versus horizontal position) or muscle velocity conditions,

may factor into the optimal stimulation pattern. The developed approach in this letter could also be applied to arm tracking for any such state dependent switching strategy.

The results of this letter establish a means for a longitudinal study in a clinical population to determine rehabilitative outcomes of maximizing torque production throughout the range of motion. Causing biceps contractions in both arms separately yields the opportunity for individuals with significant asymmetry in the upper limbs (e.g., hemiparetic stroke) to improve their strength balance. However, implementing this controller on people with neurological conditions may present additional challenges not considered in this letter, such as variations in patient sensitivity to FES. Future efforts could also investigate more complex models that capture fatigue effects which could lead to altered switching conditions.

APPENDIX

Let $V : \mathbb{R}^2 \to \mathbb{R}$ be a continuously differentiable, positive definite, common Lyapunov function candidate defined as

$$V(t) \triangleq \frac{1}{2}e_1^2(t) + \frac{1}{2}Me_2^2(t), \qquad (14)$$

which satisfies the following inequalities:

$$\lambda_1 ||z(t)||^2 \le V(t) \le \lambda_2 ||z(t)||^2, \qquad (15)$$

where $\lambda_1, \lambda_2 \in \mathbb{R}_{>0}$ are positive constants defined as $\lambda_1 \triangleq \min\left(\frac{1}{2}, \frac{c_m}{2}\right)$, $\lambda_2 \triangleq \max\left(\frac{1}{2}, \frac{c_M}{2}\right)$. Because of the signum function in the closed-loop error system in (10) and the fact that Ω_σ is a piecewise differentiable function with respect to time as the forearm changes position, the time derivative of (14) exists almost everywhere (a.e.) (i.e., $\dot{V} \overset{a.e.}{\in} \dot{\tilde{V}}$ [30]) where

$$\dot{\tilde{V}}(t) = e_1(t)(e_2(t) - \alpha e_1(t)) + e_2(t)\chi(q(t), \dot{q}(t), t)$$
$$- e_2(t)e_1(t) - K\Big[k_1\Omega_\sigma e_2^2(t) + k_2\Omega_\sigma\Big(c_3 + c_4 \parallel z(t) \parallel$$
$$+ c_5 \parallel z(t) \parallel^2\Big)e_2(t)sgn(e_2(t))\Big], \qquad (16)$$

and $K[\cdot]$ is defined in [31], which establishes a solution for time derivatives that exist a.e. After cancelling common terms and using the result of [31], (16) can be upper bounded as[4]

$$\dot{\tilde{V}}(t) \le -\alpha e_1^2(t) + |\chi(q(t), \dot{q}(t), t)||e_2(t)| - c_1 k_1 e_2^2(t)$$
$$- c_1 k_2\Big(c_3 + c_4 \parallel z(t) \parallel + c_5 \parallel z(t) \parallel^2\Big)|e_2(t)|. \quad (17)$$

Using (8), and provided the gain condition in (13) is satisfied, (12) can be used to conclude that

$$\dot{V}(t) \overset{a.e.}{\le} -\lambda_s V(t). \qquad (18)$$

Although the inequality exists a.e., due to monotonicity of Lebesgue integration, (14) can be bounded as[5]

$$V(t) \le V(t_0)\exp[-\lambda_s(t - t_0)]. \qquad (19)$$

---

[4]There is an abuse of notation since $\dot{\tilde{V}}$ is a set and the right hand side of (14) is a singleton. By this, it is meant that every member of $\dot{\tilde{V}}$ is bounded by the right hand side.

[5]The exponential decay rate λ_s represents the most conservative (i.e., smallest) decay rate for the closed-loop, switched error system. In practice, each subsystem has its own decay rate, but in the preceding stability analysis, c_1 was used as the lower bound on Ω_i for all $i \in S$.

Using (15) to further bound (19) and performing some algebraic manipulation yields (11).

REFERENCES

[1] M. Gobbo, P. Gaffurini, L. Bissolotti, F. Esposito, and C. Orizio, "Transcutaneous neuromuscular electrical stimulation: Influence of electrode positioning and stimulus amplitude settings on muscle response," *Eur. J. Appl. Physiol.*, vol. 111, no. 10, pp. 2451–2459, 2011.

[2] M. Gobbo, N. A. Maffiuletti, C. Orizio, and M. A. Minetto, "Muscle motor point identification is essential for optimizing neuromuscular electrical stimulation use," *J. Neuroeng. Rehabil.*, vol. 11, no. 1, p. 17, 2014.

[3] R. Garnett and J. Stephens, "Changes in the recruitment threshold of motor units produced by cutaneous stimulation in man," *J. Physiol.*, vol. 311, pp. 463–473, Feb. 1981.

[4] N. A. Maffiuletti, "Physiological and methodological considerations for the use of neuromuscular electrical stimulation," *Eur. J. Appl. Physiol.*, vol. 110, no. 2, pp. 223–234, Dec. 2010.

[5] R. J. Downey, M. J. Bellman, H. Kawai, C. M. Gregory, and W. E. Dixon, "Comparing the induced muscle fatigue between asynchronous and synchronous electrical stimulation in able-bodied and spinal cord injured populations," *IEEE Trans. Neural Syst. Rehabil. Eng.*, vol. 23, no. 6, pp. 964–972, Nov. 2015.

[6] R. Nguyen, K. Masani, S. Micera, M. Morari, and M. R. Popovic, "Spatially distributed sequential stimulation reduces fatigue in paralyzed triceps surae muscles: A case study," *Artif. Organs*, vol. 35, no. 12, pp. 1174–1180, 2011.

[7] R. J. Downey, T.-H. Cheng, M. J. Bellman, and W. E. Dixon, "Closed-loop asynchronous neuromuscular electrical stimulation prolongs functional movements in the lower body," *IEEE Trans. Neural Syst. Rehabil. Eng.*, vol. 23, no. 6, pp. 1117–1127, Nov. 2015.

[8] M. Goffredo *et al.*, "A two-step model to optimise transcutaneous electrical stimulation of the human upper arm," *Int. J. Comput. Math. Elect. Electron. Eng.*, vol. 33, no. 4, pp. 1329–1345, 2014.

[9] N. Malešević, L. Z. Popović, G. Bijelić, and G. Kvaščev, "Muscle twitch responses for shaping the multi-pad electrode for functional electrical stimulation," *J. Autom. Control*, vol. 20, no. 1, pp. 53–58, 2010.

[10] N. M. Malešević *et al.*, "A multi-pad electrode based functional electrical stimulation system for restoration of grasp," *J. Neuroeng. Rehabil.*, vol. 9, no. 1, p. 66, 2012.

[11] D. B. Popović and M. B. Popović, "Automatic determination of the optimal shape of a surface electrode: Selective stimulation," *J. Neurosci. Methods*, vol. 178, no. 1, pp. 174–181, Mar. 2009.

[12] A. Popović-Bijelić *et al.*, "Multi-field surface electrode for selective electrical stimulation," *Artif. Organs*, vol. 29, no. 6, pp. 448–452, 2005.

[13] C. T. Freeman, "Electrode array-based electrical stimulation using ILC with restricted input subspace," *Control Eng. Pract.*, vol. 23, no. 1, pp. 32–43, Feb. 2014.

[14] C. Salchow, M. Valtin, T. Seel, and S. Schauer, "A new semi-automatic approach to find suitable virtual electrodes in arrays using an interpolation strategy," *Eur. J. Trans. Myol.*, vol. 26, no. 2, p. 6029, Jun. 2016.

[15] P. Gad *et al.*, "Development of a multi-electrode array for spinal cord epidural stimulation to facilitate stepping and standing after a complete spinal cord injury in adult rats," *J. Neuroeng. Rehabil.*, vol. 10, no. 2, pp. 1–17, 2013.

[16] D. J. Pons, C. L. Vaughan, and G. G. Jaros, "Cycling device powered by the electrically stimulated muscles of paraplegics," *Med. Biol. Eng. Comput.*, vol. 27, no. 1, pp. 1–7, 1989.

[17] L. M. Schutte, M. M. Rodgers, F. E. Zajac, and R. M. Glaser, "Improving the efficacy of electrical stimulation-induced leg cycle ergometry: An analysis based on a dynamic musculoskeletal model," *IEEE Trans. Neural Syst. Rehabil. Eng.*, vol. 1, no. 2, pp. 109–125, Jun. 1993.

[18] M. Gföhler *et al.*, "Test bed with force-measuring crank for static and dynamic investigations on cycling by means of functional electrical stimulation," *IEEE Trans. Neural Syst. Rehabil. Eng.*, vol. 9, no. 2, pp. 169–180, Jun. 2001.

[19] J. S. Petrofsky, "New algorithm to control a cycle ergometer using electrical stimulation," *Med. Biol. Eng. Comput.*, vol. 41, no. 1, pp. 18–27, Jan. 2003.

[20] K. J. Hunt *et al.*, "Control strategies for integration of electric motor assist and functional electrical stimulation in paraplegic cycling: Utility for exercise testing and mobile cycling," *IEEE Trans. Neural Syst. Rehabil. Eng.*, vol. 12, no. 1, pp. 89–101, Mar. 2004.

[21] M. J. Bellman, T.-H. Cheng, R. J. Downey, and W. E. Dixon, "Stationary cycling induced by switched functional electrical stimulation control," in *Proc. Amer. Control Conf.*, Portland, OR, USA, 2014, pp. 4802–4809.

[22] H. Kawai, M. J. Bellman, R. J. Downey, and W. E. Dixon, "Tracking control for FES-cycling based on force direction efficiency with antagonistic bi-articular muscles," in *Proc. Amer. Control Conf.*, Portland, OR, USA, 2014, pp. 5484–5489.

[23] C. A. Rouse, A. Parikh, V. Duenas, C. Cousin, and W. E. Dixon, "Compensating for changing muscle geometry of the biceps brachii during neuromuscular electrical stimulation: A switched systems approach," in *Proc. IEEE Conf. Decis. Control*, Las Vegas, NV, USA, 2016, pp. 1328–1333.

[24] N. Sharma, K. Stegath, C. M. Gregory, and W. E. Dixon, "Nonlinear neuromuscular electrical stimulation tracking control of a human limb," *IEEE Trans. Neural Syst. Rehabil. Eng.*, vol. 17, no. 6, pp. 576–584, Dec. 2009.

[25] T. Watanabe, R. Futami, N. Hoshimiya, and Y. Handa, "An approach to a muscle model with a stimulus frequency-force relationship for FES applications," *IEEE Trans. Rehabil. Eng.*, vol. 7, no. 1, pp. 12–18, Mar. 1999.

[26] D. Liberzon, *Switching in Systems and Control*. Boston, MA, USA: Birkhäuser, 2003.

[27] T. Schauer *et al.*, "Online identification and nonlinear control of the electrically stimulated quadriceps muscle," *Control Eng. Pract.*, vol. 13, no. 9, pp. 1207–1219, Sep. 2005.

[28] M. Ferrarin and A. Pedotti, "The relationship between electrical stimulus and joint torque: A dynamic model," *IEEE Trans. Rehabil. Eng.*, vol. 8, no. 3, pp. 342–352, Sep. 2000.

[29] N. Sharma, C. M. Gregory, and W. E. Dixon, "Predictor-based compensation for electromechanical delay during neuromuscular electrical stimulation," *IEEE Trans. Neural Syst. Rehabil. Eng.*, vol. 19, no. 6, pp. 601–611, Dec. 2011.

[30] N. Fischer, R. Kamalapurkar, and W. E. Dixon, "LaSalle-Yoshizawa corollaries for nonsmooth systems," *IEEE Trans. Autom. Control*, vol. 58, no. 9, pp. 2333–2338, Sep. 2013.

[31] B. E. Paden and S. S. Sastry, "A calculus for computing Filippov's differential inclusion with application to the variable structure control of robot manipulators," *IEEE Trans. Circuits Syst.*, vol. CS-34, no. 1, pp. 73–82, Jan. 1987.